Experimental Section

Compounds. The synthesis of the compounds followed standard procedures and deuteration was mostly achieved by deuteriolysis of organometallic precursors with D_2O or deuterated acid. The following reaction pathways were used. **1**: from β-phenylethylmagnesium bromide. **2**,[27] **3**: from phenylacetylene with *n*-butyllithium followed by deuteriolysis. **4**: from **3** following ref 27. **5**: 1-phenylethanol-*1*-d_1 was prepared from acetophenone with $LiAlD_4$ and dehydrated by destillation over $KHSO_4$. **6**: from **2** by Simmons-Smith reaction[28] with CH_3I. **7**: from **4** as before. **8**: from phenylcyclopropane by reaction with NaH in Me_2SO-d_6. Ethane-d_1: from ethyl magnesium bromide by deuteriolysis. Ethylene-d_1: from vinyl magnesium bromide as before. Acetylene-d_1: from CaC_2 as before. In the last three cases the 3:1 mixture of deuterated and isotope-free material was directly prepared by reaction with D_2O/H_2O (3:1). The gaseous products were passed through two cooling traps (−50 °C) in order to remove solvent traces and condensed into the NMR tube filled with the appropriate solvent (see below). In the case of acetylene the product mixture contained C_2H_2, C_2HD, and C_2D_2 in a ratio of 1:2:2 as determined by integration of the ^1H-decoupled ^{13}C NMR spectrum. The deuterated methylmethanes as well as the deuterated *n*-alkanes were prepared via the corresponding Grignard compounds, while the phenylmethanes were generated from benzylmagnesium chloride, diphenylmethyllithium, and triphenylmethylmagnesium bromide, respectively, by deuteriolysis.

Spectra. ^{13}C NMR spectra were measured under ^1H broadband decoupling at 100.61 MHz on a Bruker WH-400 FT NMR spectrometer equipped with an ASPECT 2000 data system. Isotope shifts were determined from 3:1 or 4:1 mixtures of deuterated and isotope-free material either prepared directly or by mixing. Ethane and ethylene were measured at 173 K in CD_2Cl_2/CS_2 (20 vol %), while acetylene was measured at 213 K in acetone-d_6 (50 vol %). All other compounds were measured as 1 M solutions in $CDCl_3$ (1% Me_4Si) at 310 K, except for propane and butane, which were measured at 215 and 265 K, respectively. Spectral assignments were available from the literature[22a,29] and supported by intensity ratios and line splittings due to $^{13}C,^2H$ spin-spin coupling. Ambiguities in the assignments of isotope shifts were removed by increasing the concentration of one of the components in the test mixture. In order to achieve highest possible resolution, selected portions of the spectrum were recorded separately with use of sweep widths of 100-300 Hz and zero-filling resulting in an experimental error of $<\pm 0.5$ ppb for the isotope shifts and $>\pm 0.05$ Hz for the coupling constants. Where necessary, resolution enhancement and/or ^2H decoupling was employed in order to remove signal overlap due to line-broadening effects.

Acknowledgment. We are indebted to the Deutsche Forschungsgemeinschaft and the Fonds der Chemischen Industrie, Frankfurt, for generous support of our research.

Registry No. Ethylbenzene, 100-41-4; styrene, 100-42-5; phenylacetylene, 536-74-3; phenylcyclopropane, 873-49-4; heptane, 142-82-5; octane, 111-65-9; nonane, 111-84-2; decane, 124-18-5; methane, 74-82-8; ethane, 74-84-0; propane, 74-98-6; butane, 106-97-8; pentane, 109-66-0; hexane, 110-54-3; deuterium, 7782-39-0.

(27) Quintard, J. P.; Pereyre, M. I. *J. Labelled Compd.* **1978**, *14*, 653.
(28) Simmons, H. E.; Smith, R. D. *J. Am. Chem. Soc.* **1958**, *80*, 5323; **1959**, *81*, 4256.
(29) Bremser, W.; Ernst, L.; Franke, B.; Gerhards, R.; Hardt, A. "Carbon-13 NMR Spectral Data", 3rd ed.; Verlag Chemie: Weinheim, 1981.

Dynamics of Phenylalanine in the Solid State by NMR

M. H. Frey,† J. A. DiVerdi,‡ and S. J. Opella*

Contribution from the Department of Chemistry, University of Pennsylvania, Philadelphia, Pennsylvania 19104. *Received April 19, 1985*

Abstract: The dynamics of the amino acid phenylalanine in the solid state at room temperature are characterized by ^2H and ^{13}C NMR experiments. Samples crystallized from water at neutral pH and samples crystallized from ethanol/water solution have two identifiable types of molecules. About half of the phenylalanine molecules crystallized from water have immobile rings, and the rest have rings that undergo rapid 2-fold flips about the C_β-C_γ bond axis. Analysis of the ^2H and ^{13}C relaxation rates indicates that the frequency of ring flips for phenylalanine crystallized from water is approximately 10^9 Hz. Both types of phenyl rings in the sample crystallized from ethanol/water are immobile on time scales slower than about 10^2 Hz. In contrast, phenylalanine hydrochloride samples have only a single type of molecule with a ring undergoing relatively slow ($\approx 10^2$ Hz) reorientation about the C_β-C_γ bond axis.

Large amplitude motions are present in many crystalline and amorphous solid materials at room temperature.[1] These motions can be readily characterized by solid-state NMR because motional averaging strongly influences spectral manifestations of the nuclear spin interactions. A wide range of amplitudes and frequencies of intramolecular motions can be examined through experiments that measure spectroscopic properties of the chemical shift, dipolar, and quadrupolar interactions.

In solid-state NMR, the amplitudes and directions of rapid motions can be deduced from the analysis of powder pattern line shapes. Motions alter powder patterns through the averaging of the spin interaction tensors. The effects of specific types of motions on powder pattern line shapes can be readily calculated when these motions occur frequently compared to the NMR time scale defined by the frequency breadth of the static powder pattern resulting from the spin interaction. Isotropic chemical shift spectra typically reflect motions slower than about 10^2 Hz, chemical shift anisotropy powder patterns are averaged by motions that occur more rapidly than 10^3 Hz, ^1H-^{13}C heteronuclear dipolar couplings are averaged by motions faster than 10^4 Hz, and the ^2H quadrupole interaction is sensitive to motions that are faster than 10^6 Hz. Relaxation measurements reflect events that occur near the 10^9-Hz Larmor frequencies. The averaging of powder patterns requires large amplitude fluctuations, while efficient relaxation can be induced by both relatively small as well as large amplitude fluctuations.

The dynamics of phenylalanine in the solid state are suprisingly complex.[2,3,5,11] The phenyl side chains of the aromatic amino

† Present address: JEOL (USA), Inc., Peabody, MA 01960.
‡ Present address: Smith, Kline & French Laboratories, Philadelphia, PA 19101.

(1) For reviews see: (a) Torchia, D. A. *Annu. Rev. Biophys. Bioeng.* **1984**, *13*, 125-144. (b) Opella, S. J. *Methods Enzymol.*, in press.
(2) Gall, C. M.; DiVerdi, J. A.; Opella, S. J. *J. Am. Chem. Soc.* **1981**, *103*, 5039-5043.
(3) Kinsey, R. A.; Kintanar, A.; Oldfield, E. *J. Biol. Chem.* **1981**, *256*, 9028-9036.
(4) Rice, D. M.; Wittebort, R. J.; Griffin, R. G.; Meirovitch, E.; Stimson, E. R.; Meinwald, Y. C.; Freed, J. H.; Scheraga, H. A. *J. Am. Chem. Soc.* **1981**, *103*, 7707-7710.

0002-7863/85/1507-7311$01.50/0

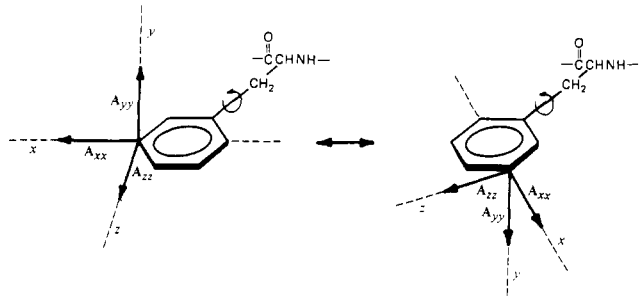

Figure 1. Effect of 180° ring flips about the C_β–C_γ bond axis on the orientation of the general spin interaction tensor in the phenyl ring.

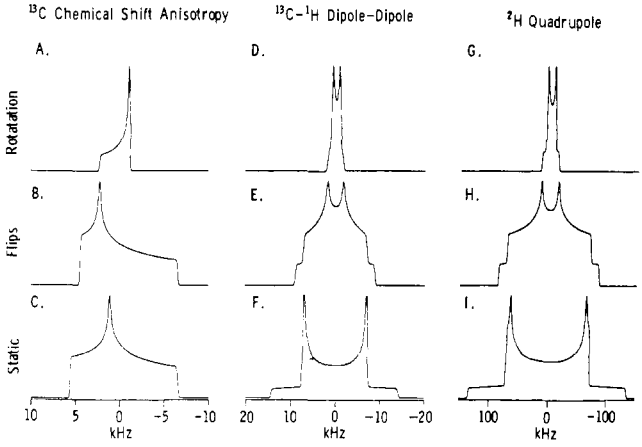

Figure 2. Calculated powder patterns for the three spin interactions described by the tensor shown in Figure 1.

acids phenylalanine and tyrosine undergo 2-fold jumps about the C_β–C_γ bond axis in a variety of solid samples including the free amino acids, small natural and synthetic peptides, and proteins.[2-12] The motions present in three different types of solid phenylalanine samples are described here. The phenylalanine samples were obtained as powders of (1) crystals of zwitterions from water at neutral pH, (2) crystals from an ethanol/water solution, and (3) crystals of the hydrochloride salt. Figure 1 illustrates how 180° reorientation about the C_β–C_γ bond axis affects the orientation of the principal axes of a generalized tensor, A, in the ring of phenylalanine.[7] This tensor has the same orientation in the molecular frame for the ^{13}C chemical shift, ^1H–^{13}C dipole–dipole, and ^2H quadrupole spin interactions.[13,14] However, the magnitudes of the principal elements are different for each of these interactions. Calculated powder patterns for the δ and ϵ ring sites are shown in Figure 2 for each of the interactions for three limiting cases of ring motion about the C_β–C_γ bond axis: (1) immobile (static) ring, (2) 2-fold (180°) ring flips, and (3) continuous rotational diffusion of the ring. Clearly, these three limiting possibilities can be distinguished by comparing experimental line shapes to those calculated for the models of motion.

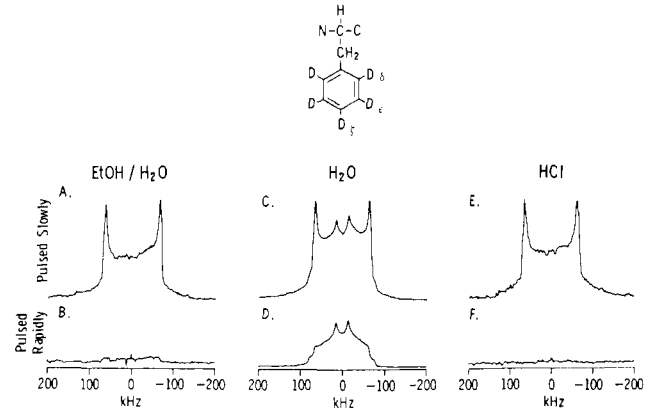

Figure 3. ^2H NMR spectra of the three types of solid phenylalanine-d_5 samples. All spectra were obtained by using the quadrupole echo pulse sequence. The recycle delay was 15 s for the top row (A, C, and E) and 0.1 s for the bottom row (B, D, and F) of spectra.

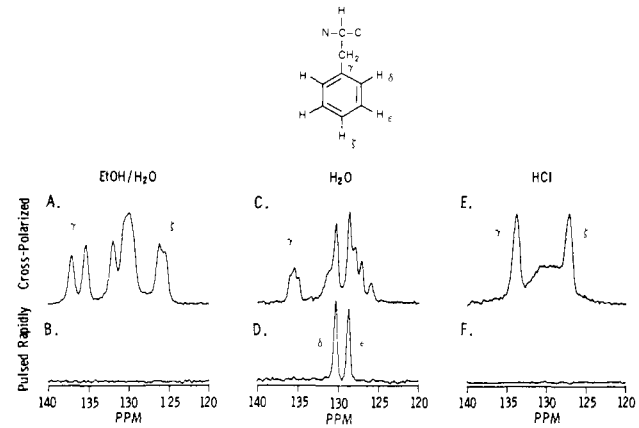

Figure 4. ^{13}C NMR spectra of the aromatic carbon resonance region of the three types of solid phenylalanine samples. All spectra were obtained by using magic-angle sample spinning and high-power proton decoupling during acquisition. Cross-polarization was used to develop transverse magnetization for the spectra in the top row (A, C, and E).

Experimental Section

L-Phenylalanine was obtained from Sigma (St. Louis, MO) and crystallized from saturated, refluxing solutions of (1) water at neutral pH, (2) 1:1 (v/v) ethanol/water solution, and (3) concentrated hydrochloric acid. L-[2′,3′,4′,5′,6′-$^2H_5$]phenylalanine (phenylalanine-d_5) was prepared as described previously[15] and crystallized in the same ways as the unlabeled phenylalanine samples.

The NMR experiments were performed on homebuilt double-resonance spectrometers operating at magnetic fields of 3.5 and 5.9 T. All experiments were performed at room temperature. The isotropic ^{13}C chemical shift spectra were obtained at 68 MHz; the samples were rotated at ≈4 KHz in Andrew-Beams rotors at the magic angle (54.7°) with respect to the applied magnetic field. The cross-polarized spectra employed a 1-ms mixing period, and phase cycling was used to reduce artifacts. A 2.5-mT proton decoupling field was applied during data acquisition. The spectra demonstrating spinning sidebands were acquired with a 1.9-kHz spin rate. In some spectra, $\pi/2$ pulses were used with a short recycling time instead of cross-polarization in order to select for spins with short T_1s. ^{13}C T_1s were measured by saturating the ^{13}C magnetization with a burst of randomly phased pulses and following its recovery at various times with a $\pi/2$ read pulse. Proton decoupling was applied only during the data acquisition period. In some experiments, low-power proton irradiation (≈0.1 mT) was applied continuously during the recovery period as well.

The ^2H NMR spectra were obtained at 38 MHz in a magnetic field of 5.9 T by using a quadrupole echo pulse sequence[16] with an interpulse

(5) Rice, D. M.; Blume, A.; Hertzfeld, J.; Wittebort, R. J.; Huang, T. H.; DasGupta, S. K.; Griffin, R. G. *Biomol. Stereodyn.* **1981**, 255–270.
(6) Schramm, S.; Kinsey, R. A.; Kintanar, A.; Rothgeb, T. M.; Oldfield, E. *Biomol. Stereodyn.* **1981**, 271–286.
(7) Gall, C. M.; Cross, T. A.; DiVerdi, J. A.; Opella, S. J. *Proc. Natl. Acad. Sci. U.S.A.* **1982**, *79*, 101–105.
(8) Gierasch, L. M.; Frey, M. H.; Hexem, J. G.; Opella, S. J. *ACS Symp. Ser.* **1982**, *No. 191*, 233–247.
(9) Gierasch, L. M.; Opella, S. J.; Frey, M. H. *Pept.: Synth., Struct., Funct., Proc. Am. Pept. Symp., 7th* **1981**, 267–275.
(10) Frey, M. H.; Hexem, J. G.; Leo, G. C.; Tsang, P.; Opella, S. J.; Rockwell, A. L.; Gierasch, L. M. *Pept.: Synth., Struct., Funct., Proc. Am. Pept. Symp., 8th* **1983**, 763–771.
(11) Schaefer, J.; Stejskal, E. O.; McKay, R. A.; Dixon, W. T. *J. Magn. Reson.* **1984**, *57*, 85–92.
(12) Frey, M. H.; Opella, S. J.; Rockwell, A. L.; Giersch, L. M. *J. Am. Chem. Soc.* **1985**, *107*, 1946–1951.
(13) Pausak, S.; Tegenfeldt, J.; Waugh, J. S. *J. Chem. Phys.* **1974**, *61*, 1338–1344.
(14) Barnes, R. G.; Bloom, J. W. *J. Chem. Phys.* **1972**, *57*, 3082–3086.
(15) Matthew, H. R.; Matthew, K. S.; Opella, S. J. *Biochim. Biophys. Acta* **1977**, *497*, 1–13.

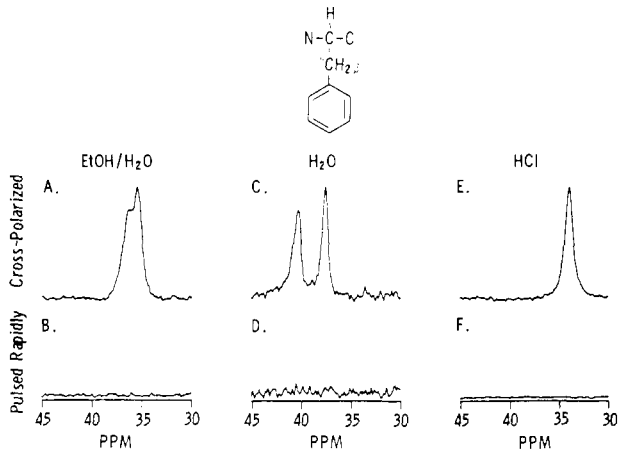

Figure 5. ^{13}C NMR spectra of the β-carbon resonance region of the three types of solid phenylalanine samples. Conditions were the same as in Figure 4.

spacing of 50 μs. ^2H T_1s were measured by applying a burst of randomly phased pulses to saturate the ^2H spins; recovery of the magnetization at various times was followed by using the usual quadrupolar echo sequence.

Two-dimensional magic angle spinning separated local field spectra were obtained as described previously[17] by using continuous off-resonance decoupling to reduce the broadening effects in the ω_1 dimension from ^1H–^1H homonuclear dipolar broadening.[17] The scaling factor was set experimentally to be 0.72 in order to increase the number of spinning sidebands observed for data analysis. The intensities of the sidebands were highly reproducible; however, the intensities of the center bands were found to vary because dc offsets in the dipolar (t_1) free induction decays affected the intensity a zero frequency after base-line corrections in the data processing. Therefore, all interpretations are based on comparisons of sideband intensities.

Results

Comparisons. The spectral comparisons in Figures 3, 4, and 5 clearly illustrate the complexities of solid-state NMR spectroscopy of the various phenylalanine preparations. The spectra in the top rows of these figures have intensity from all spins in the samples, while the spectra in the bottom rows have intensity from only those spins which have short T_1s. ^2H NMR spectra from the three samples of phenylalanine-d_5 are in Figure 3. The spectra in the top row are from spins that are fully relaxed since they were obtained with long recycle delays; therefore, all the spins in each sample are represented with equivalent intensity regardless of any T_1 differences. The spectra in the bottom row were obtained with short recycle delays so that signals from spins with long T_1 are suppressed and the spectra represent only those spins with short T_1. Figures 4 and 5 contain high-resolution natural-abundance ^{13}C NMR spectra of phenylalanine samples similar to those used to obtain the results shown in Figure 3. The spectra in the top row were obtained by cross-polarization and contain resonance intensity from all carbons. The spectra in the bottom row were obtained by rapid pulsing at the ^{13}C resonance frequency; therefore, only spins with short T_1 appear in these spectra. Phenylalanine contains only a single β carbon, yet the spectra in Figures 5A and 5C show clear evidence of two peaks while Figure 5E contains a single line as expected.

Phenylalanine from Ethanol/Water. The phenylalanine sample crystallized from ethanol/water has no signals with short T_1 based on the lack of ^2H intensity in Figure 3B or of ^{13}C intensity in Figures 4B and 5B. The high-resolution ^{13}C NMR spectrum in Figure 4A obtained by cross-polarization indicates that there are two types of phenylalanine molecules in the sample, since there are two clearly distinguishable C_γ resonances and two partially resolved C_ζ resonances in the aromatic region. This conclusion is reinforced by the two partially resolved C_β resonances in Figure 5A. Both types of phenylalanine molecules present in the sample crystallized from ethanol/water have immobile rings as demonstrated by the unaveraged ^2H powder patterns with long T_1 in Figure 3 and the long T_1 of all carbon sites as shown in Figures 4B and 5B.

Phenylalanine from Water. The phenylalanine sample crystallized from water at neutral pH also shows evidence of two types of molecules. There are two distinct C_β resonances of similar intensity in Figure 5C, and the aromatic region in Figure 4C contains too many resonances to be accounted for by a single type of molecule, even one that is immobile with distinct chemical shifts for each ring site. The ^{13}C NMR spectrum in Figure 4D is from C_δ and C_ϵ sites with short T_1. Even though each ring can have two C_δ and two C_ϵ resonances, they are each averaged by motion to single lines in this spectrum. The lines with short T_1 are assigned to the δ and ϵ sites, since the motions apparent from the ^2H NMR spectra can only influence these sites and their resonance frequencies are similar to those observed for these sites in solution. The ^2H NMR spectra for this type of sample (Figure 3C and 3D) have been fully described previously.[2] There is a short T_1 component in the powder pattern from the δ and ϵ deuterons undergoing rapid 2-fold flips. There is also a component in the powder pattern from the ζ deuterons in the flipping rings with long T_1s since these deuterons are not affected by motions about the C_β–C_γ bond axis. In addition, there is a long T_1 component from all ring deuterons in molecules with rings not undergoing rapid motion. All of the long T_1 components have the unaveraged powder pattern line shapes characteristic of static C–D bonds. Therefore, the ^2H spectrum in Figure 3C is the sum of both flip-averaged (short T_1) and static (long T_1) powder patterns. There are clearly two approximately equal populations of molecules in phenylalanine crystallized from water: one type undergoing rapid ring flips and the other type with rigid rings. The two different types of dynamics reflected in the line shapes and relaxation rates of the deuterons and the relaxation rates of the carbons are consistent with the two different environments reflected in the ^{13}C chemical shifts of aromatic and C_β resonances.

Phenylalanine Hydrochloride. The data for the phenylalanine hydrochloride samples are most simply interpreted in terms of a single class of molecules. The unaveraged ^2H powder pattern of Figure 3E shows that all the rings sites are rigid on the 10^6-Hz time scale defined by the ^2H NMR experiment. The absence of observable signals in Figure 3F results from the long T_1 of the sites in rigid rings. The single-line C_β resonance in Figure 5E is in contrast to the two C_β resonances for the other phenylalanine samples. The aromatic region of the ^{13}C spectrum in Figure 4E is quite unusual in appearance. There are single narrow lines from the C_γ and C_ζ sites, but a broad peak arises from the C_δ and C_ϵ sites. The C_γ resonance is assigned based on an experiment showing it to be from a carbon without a directly bonded proton, and the C_ζ resonances is assigned based on its upfield position and the lack of perturbation by the ring motions. These results suggest that the rings in phenylalanine hydrochloride have motions about the C_β–C_γ bond axis that leave the C_β, C_γ, and C_ζ resonances unaffected. These motions apparently occur on the 10^1–10^2-Hz time scale necessary for intermediate exchange broadening of the isotropic C_δ and C_ϵ ring resonances. This is fully consistent with the ^2H NMR results, since motions on this time scale do not occur frequently enough to influence the ^2H line shapes.

Analysis of Chemical Shift and Dipolar Sidebands in Magic Angle Spinning Experiments. The line shapes from two other spin interactions are available for analysis of ring dynamics. The ^{13}C chemical shift anisotropy and the ^1H–^{13}C dipole–dipole interactions are used to illustrate the comparisons possible between static and flipping ring sites in phenylalanine crystallized from water. Figure 6B shows the spinning sidebands derived from ^{13}C chemical shift anisotropy interaction in a sample rotating relatively slowly at the magic angle. The signals were obtained from $\pi/2$ pulses at the ^{13}C resonance frequency with a short recycle time so they correspond only to the rapidly flipping C_δ and C_ϵ sites in the sample. The center band is equivalent to that of Figure 4D. The ^{13}C chemical shift powder patterns can be reconstructed from the spinning sideband intensities by using a moment analysis.[18] Figure

(16) Davis, J. H.; Jeffery, K. R.; Bloom, M.; Vlaic, M. I.; Higgs, T. P. *Chem. Phys. Lett.* **1976**, *42*, 390–395.
(17) Maricq, M. M.; Waugh, J. S. *J. Chem. Phys.* **1983**, *70*, 3300–3316.

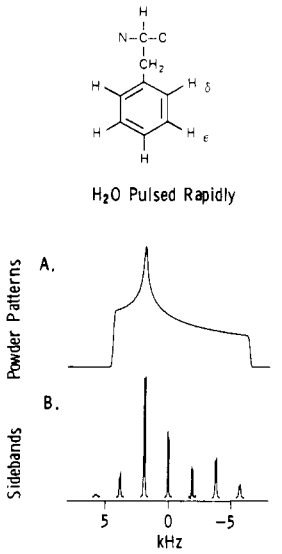

Figure 6. ^{13}C NMR spectra of the aromatic carbon resonance region of the phenylalanine sample crystallized from water at neutral pH obtained with direct pulsing with a 0.75-s recycle delay at a field strength of 5.9 T with a relatively slow spinning rate of 1.9 kHz. B is the experimental spectrum and A is the calculated spectrum based on the parameters of the static powder pattern in Figure 2C.

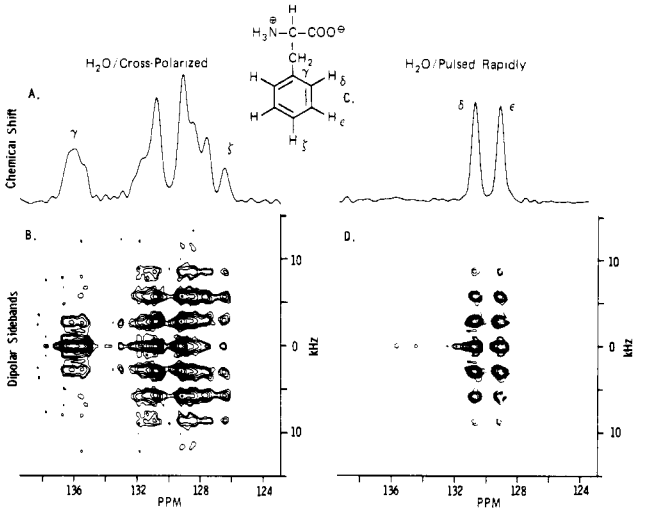

Figure 7. Separated local field spectra of phenylalanine crystallized from water. The spectra on the left were obtained by using cross-polarization to develop transverse magnetization. The spectra on the right were obtained with direct pulsing. Isotropic chemical shift spectra are aligned along the top.

6A contains the powder pattern derived from the sideband intensities of Figure 6B. This pattern is similar to that calculated for flipping C_δ and C_ϵ sites in Figure 2B and substantially different from patterns expected for freely rotating (Figure 2A) or static (Figure 2C) rings. The chemical shift powder pattern comparison between the experimentally derived pattern (Figure 6A) and the calculated motionally averaged pattern (Figure 2B) demonstrates that the sites with short T_1 in phenylalanine crystallized from water are undergoing flip motions.

Two-dimensional magic angle spinning separated local field spectra have the ^{13}C isotropic chemical shift interaction in one dimension and the scaled ^1H–^{13}C dipole–dipole interaction in the second dimension. Figure 7A is the one-dimensional aromatic ^{13}C chemical shift spectrum while Figure 7B is a two-dimensional contour plot of the ^{13}C isotropic chemical shift vs. the ^1H–^{13}C dipolar spinning sidebands. Both were obtained by using cross-polarization to develop the ^{13}C magnetization. The corresponding

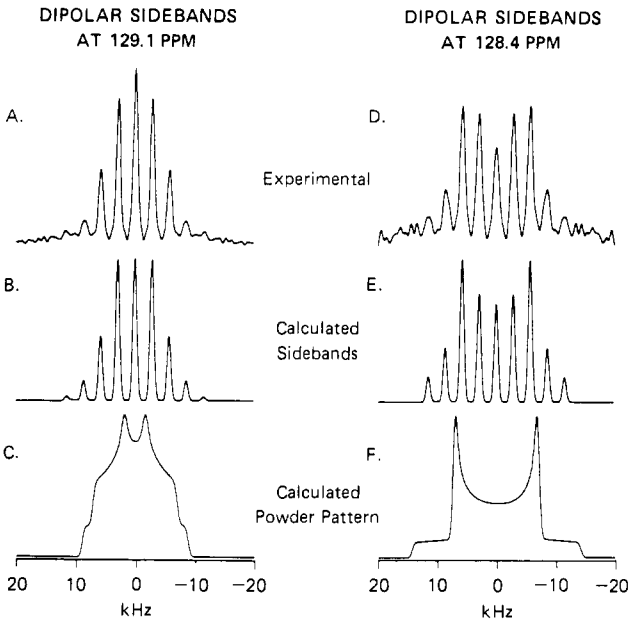

Figure 8. Selected columns from the two-dimensional data sets in Figure 7. A corresponds to 129.1 ppm and D corresponds to 128.4 ppm. B and E are the sideband intensities calculated based on the parameters of the flip averaged powder pattern C and the static powder pattern F, respectively, taking into account the experimental spinning rate and scaling factor.

spectra obtained by developing the ^{13}C magnetization using direct pulsing with a short recycle delay to select for those carbons with short T_1s are illustrated in Figure 7C and 7D. The contour plots demonstrate a high degree of resolution in the ^{13}C isotropic chemical shift dimension and well-resolved spinning sidebands in the ^1H–^{13}C dipolar dimension. To analyze the effects of motion in the ^1H–^{13}C dipolar interaction, it is necessary to look at cross sections parallel to the dipolar (ω_1) axis as shown in Figure 8. The intensities of the spinning sidebands for a cross section through a resonance from an immobile site at 126.4 ppm were analyzed to yield a C–H bond length of 1.15 ± 0.05 Å. This value was then used to reconstruct the corresponding static powder pattern (Figure 8F) and the corresponding static spinning sideband intensities (Figure 8E). This static tensor was averaged over a 180° flip motion, yielding the powder pattern and sideband intensities in Figure 8B and 8C. The comparisons between the experimental and calculated dipolar sideband intensities for a flip-averaged site at 129.1 ppm (Figure 8A and 8B) and a static site at 128.4 ppm (Figure 8D and 8E) show very good agreement in spite of limited chemical shift resolution. This experiment shows that there are two types of ring carbons with similar isotropic chemical shifts: those that are static on the 10^4-Hz time scale and those that execute 180° flips more rapidly than 10^4 Hz.

The powder pattern line-shape analysis for the anisotropic chemical shift, dipolar, and quadrupolar interactions indicate that the phenylalanine sample crystallized from water at neutral pH has a substantial number of phenyl side chains that exhibit fast large amplitude motions in the form of 180° ring flips. A lower limit of 10^6 Hz for the frequency of this motion is indicated by this same analysis. The observed frequency breadth of the powder patterns of both mobile and rigid sites is reduced by a few percent from those expected from rigid lattice values;[2,11] in general, this is due to the presence of small amplitude thermal motions. Since the amplitude and direction of the large amplitude motions are established from this line-shape analysis, relaxation measurements can be used to independently determine the frequencies of those motions.

Analysis of Relaxation Measurements. The effects of specific motions on spin–lattice relaxation times are well-understood.[19,20]

(18) DiVerdi, J. A.; Opella, S. J. *J. Am. Chem. Soc.* **1982**, *104*, 1761–1762.

(19) London, R. E. *Magn. Reson. Biol.* **1980**, *1*, 1–69.
(20) Torchia, D. A.; Szabo, A. J. *J. Magn. Reson.* **1982**, *49*, 107–120.

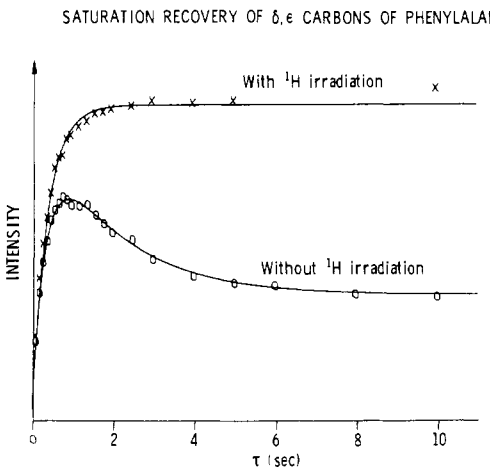

Figure 9. Experimental intensity data from recovery of ^{13}C magnetization with (X) and without (O) a proton irradiation field of 0.1 mT during the recovery interval (t) following a burst of saturating pulses.

Equation 1 describes spin–lattice relaxation due to the heteronuclear ^1H–^{13}C dipolar interaction. Equation 2 describes that

$$1/T_1^{C-H} = 1/10[\gamma C \gamma H h/r^3]^2[J(\tau,\omega_C - \omega_H) + 3J(\tau,\omega_C) + 6J(\tau,\omega_C + \omega_H)] \quad (1)$$

due to the ^2H quadrupole interaction.

$$1/T_1^Q = 2/15[e^2qQ/h]^2[J(\tau,\omega_D) + 4J(\tau,2\omega_D)] \quad (2)$$

The spectral density function ($J(\omega)$) is readily derived in the presence of magic angle spinning with $\omega_{Rot} > \Delta\omega_{CSA}, 1/T_1$. ω_C, ω_H, and ω_P are the Larmor frequencies. The quantities in the squared brackets are the effective interaction magnitudes. An orientation independent correlation function, identical with that used for solution NMR, can be applied to the analysis of ^2H relaxation provided that the integrated intensity across the powder pattern is used.

A 180° flip motion can be described as a two-site exchange with the forward and reverse frequencies equal to twice the flip frequency ($\tau_{forward} = \tau_{backward} = 2\tau_{flip}$). The spectral density function is given in eq 3 with θ being the angle between the two

$$J(\tau_F,\omega) = 3/4 \sin^2\theta(\tau_F/(1 + \omega^2\tau_F^2)) \quad (3)$$

sites, i.e., 120° for the δ and ϵ sites and 0° for the ζ site in a phenyl ring as shown in Figure 1.

The ring flips in phenylalanine recrystallized from water are very efficient in relaxing the C_δ and C_ϵ carbons but not the other ring carbons. The observed magnetization for these sites in a ^{13}C saturation recovery measurement at 3.5 T is illustrated in Figure 9. The data in the lower trace (O) were obtained in an experiment without proton irradiation during the recovery period. The loss of signal intensity (with a 1.8-s time constant) following the recovery from saturation is attributed to spin exchange from the ^{13}C spins back into the ^1H spin reservoir via the ^1H–^{13}C dipolar interaction.[21] Very low levels of irradiation at the proton frequency (≈10 W) were sufficient to eliminate this process as shown in the upper trace (X) of Figure 9. The measured single-exponential carbon T_1s for the C_δ and C_ϵ sites are the same within experimental error: 352 ± 15 ms at 5.9 T and 335 ± 15 ms at 3.5 T. The deuterium spin–lattice relaxation time for the δ and ϵ deuterons is 11 ± 2 ms. at 5.9 T. In addition to the flipping motion of the rings, it is necessary to consider the effects of small amplitude librational motions near the Larmor frequency; however, calculations show that such motions with angular dispersions as large as 20° will not reduce ^2H T_1 below 1 s. Therefore, the measured relaxation times reflect a flip rate of $\approx 10^9$ Hz by comparing the experimental rates for both carbon and deuteron sites with rates calculated as being induced by the flip motion, using the formalism described with eq 1–3.

Discussion

The complex solid-state ring dynamics of crystalline phenylalanine have been described by utilizing several different nuclear spin interactions. The type of motion was determined to be ring flips by line-shape analysis, and the frequencies of motions were found to be around 10^2 Hz for phenylalanine hydrochloride and around 10^9 Hz for phenylalanine crystallized from water by both line-shape analysis and relaxation measurements. Phenylalanine recrystallized from ethanol/water was found to contain two distinguishable types of immobile molecules. Two types of molecules were also found in phenylalanine recrystallized from water: one being immobile and the other with a rapidly flipping ring. These experiments demonstrate that the intramolecular dynamics of organic solids depends not only on the molecules themselves but also critically on the organization of the crystal lattice in which they are situated. Intermolecular associations and crystal packing forces can create complex potential energy wells which are both deep enough to prevent free rotation and shallow enough to allow thermally activated jumps like ring flips as frequently as 10^9 Hz.

Acknowledgment. This research was supported by Grants GM-24266 and GM-29754 from the N.I.H. M.H.F. was supported by a Cell and Molecular Biology Training Grant.

Registry No. L-Phenylalanine, 63-91-2; L-phenylalanine hydrochloride, 17585-69-2.

(21) Garroway, A. N.; Vanderhart, D.; Earl, W. L. *Philos. Trans. R. Soc. London* **1981**, *299*, 609–620.